

## Lagrange mesh, relativistic flux tube, and rotating string

Fabien Buisseret\* and Claude Semay†

*Groupe de Physique Nucléaire Théorique, Université de Mons-Hainaut, Académie Universitaire Wallonie-Bruxelles,  
Place du Parc 20, B-7000 Mons, Belgium*

(Received 6 September 2004; published 28 February 2005)

The Lagrange mesh method is a very accurate and simple procedure to compute eigenvalues and eigenfunctions of nonrelativistic and semirelativistic Hamiltonians. We show here that it can be used successfully to solve the equations of both the relativistic flux tube model and the rotating string model, in the symmetric case. Verifications of the convergence of the method are given.

DOI: 10.1103/PhysRevE.71.026705

PACS number(s): 02.70.-c, 03.65.Ge, 12.39.Ki, 02.30.Mv

### I. INTRODUCTION

The Lagrange mesh method is a very accurate and simple procedure to compute eigenvalues and eigenfunctions of a two-body Schrödinger equation [1–3]. The trial eigenstates are developed in a basis of well-chosen functions, the Lagrange functions, and the Hamiltonian matrix elements are obtained with a Gauss quadrature. This method can be extended to treat very accurately three-body problems, in nuclear or atomic physics [4]. Recently, it has also been successfully applied to a two-body spinless Salpeter equation [5]. The idea of this work is to adapt the Lagrange mesh method to solve the complicated equations of both the relativistic flux tube and the rotating string models.

The relativistic flux tube (RFT) is a phenomenological model describing the mesons. It relies on the assumption that the quark and the antiquark are connected by a straight color flux tube carrying both energy and momentum. The quarks are considered as spinless particles in the original version of the model [6–8]. The RFT reproduces the linear Regge trajectories, and reduces to the usual Schrödinger equation with a linear confinement potential in the nonrelativistic limit. We will consider here the particular case of mesons composed of two equal quark masses. The equations of motion of the symmetric RFT model are given by two coupled nonlinear equations: one defining the Hamiltonian and the other defining the orbital angular momentum. These equations depend on a quark transverse velocity operator and their solutions will be obtained by the use of an iterative procedure similar to the one proposed in Ref. [8].

The rotating string model (RS) also describes the mesons. It is derived from the QCD Lagrangian and is characterized by the fact that it contains auxiliary fields [9–11]. The equations of motion for this model are similar to the equations of motion of the RFT model. In the symmetric case, it has been showed that the RS is classically equivalent to the RFT if the auxiliary fields are correctly eliminated [12]. This result, extended recently to the asymmetric case [13], provides a clear physical interpretation for the characteristic variables of the RS model.

The Lagrange mesh method is explained in Sec. II. In Sec. III, the relativistic flux tube and the rotating string models are described. Then, it is shown, in Sec. IV, how the Lagrange mesh method can be applied to solve the equations of motion of these models. After some remarks, given in Sec. V, about the numerical and physical parameters, the results are presented in Sec. VI and the reliability of our numerical method is checked. Finally, some concluding remarks are given in Sec. VII.

### II. LAGRANGE MESH METHOD

A Lagrange mesh is formed on  $N$  mesh points  $x_i$  associated with an orthonormal set of indefinitely derivable functions  $f_j(x)$  [1–3]. A Lagrange function  $f_j(x)$  vanishes at all mesh points but one; it satisfies the Lagrange conditions

$$f_j(x_i) = \lambda_i^{-1/2} \delta_{ij}. \quad (1)$$

The mesh points  $x_i$ , the zeros of a particular polynomial, and the  $\lambda_i$  are connected with a Gauss quadrature formula

$$\int_a^b g(x) dx \approx \sum_{k=1}^N \lambda_k g(x_k), \quad (2)$$

used to compute all the integrals over the interval  $[a, b]$ .

As we consider only radial equations, this interval is  $[0, \infty[$ , leading to a Gauss-Laguerre quadrature. The Gauss formula (2) is exact when  $g(x)$  is a polynomial of degree  $2N-1$  at most, multiplied by  $\exp(-x)$ . The Lagrange-Laguerre mesh is then based on the zeros of the Laguerre polynomial  $L_N(x)$  of degree  $N$  [1]. An explicit form can be derived for the corresponding regularized Lagrange functions

$$f_i(x) = (-1)^i x_i^{-1/2} x(x-x_i)^{-1} L_N(x) e^{-x/2}. \quad (3)$$

To show how these elements can be applied to a physical problem, let us consider a Hamiltonian  $H=T(\vec{p}^2)+V(r)$ , where  $T(\vec{p}^2)$  is the kinetic term and  $V(r)$  a radial potential ( $\hbar=c=1$ ). The calculations are performed with trial states  $|\psi\rangle$  given by

$$|\psi\rangle = \sum_{k=1}^N C_k |f_k\rangle, \quad (4)$$

where

\*Email address: fabien.buisseret@umh.ac.be

†Email address: claude.semay@umh.ac.be

$$\langle \vec{r} | f_k \rangle = \frac{f_k(r/h)}{\sqrt{hr}} Y_{\ell m}(\hat{r}). \quad (5)$$

$\ell$  is the orbital angular momentum quantum number and the coefficients  $C_k$  are linear variational parameters.  $h$  is the scale parameter chosen to adjust the mesh to the domain of physical interest. We define  $r=hx$ , with  $x$  a dimensionless variable.

We have now to compute the Hamiltonian matrix elements. Using the properties of the Lagrange functions and the Gauss quadrature (2), the potential matrix is diagonal. Its elements are

$$\langle f_i | V(r) | f_j \rangle \approx V(hx_i) \delta_{ij}, \quad (6)$$

and only involve the value of the potential at the mesh points. As the matrix elements are computed only approximately, the variational character of the method cannot be guaranteed. But the accuracy of the method is preserved [14].

The kinetic energy operator is only a function of  $\vec{p}^2$ . Let us define the corresponding matrix,

$$P_{ij}^2 = \langle f_i | \vec{p}^2 | f_j \rangle. \quad (7)$$

It is shown in Ref. [3] that, using the Gauss quadrature and the properties of the Lagrange functions, one obtains

$$P_{ij}^2 = \frac{1}{h^2} \left( P_{r ij}^2 + \frac{\ell(\ell+1)}{x_i^2} \delta_{ij} \right), \quad (8)$$

where

$$P_{r ij}^2 = \begin{cases} (-1)^{i-j} (x_i x_j)^{-1/2} (x_i + x_j) (x_i - x_j)^{-2} & (i \neq j), \\ (12x_i^2)^{-1} [4 + (4N+2)x_i - x_i^2] & (i = j). \end{cases} \quad (9)$$

Now the kinetic energy matrix  $T(P^2)$  can be computed with the following method [5]

(1) Diagonalization of the matrix  $P^2$ . If  $D^2$  is the corresponding diagonal matrix, we have

$$P^2 = S D^2 S^{-1}, \quad (10)$$

where  $S$  is the transformation matrix.

(2) Computation of  $T(D^2)$  by taking the function  $T$  of all diagonal elements of  $D^2$ .

(3) Determination of the matrix elements  $T_{ij} = \langle f_i | T(P^2) | f_j \rangle$  in the Lagrange basis by using the transformation matrix  $S$

$$T(P^2) = S T(D^2) S^{-1}. \quad (11)$$

This procedure can easily be generalized to the case of an arbitrary function  $F$  of any given matrix  $M$ , in order to compute  $F(M)$  (provided the calculation is relevant). Note that such a calculation is not exact because the number of Lagrange functions is finite. However, it has already given good results in the semirelativistic case, where  $T(\vec{p}^2) = \sqrt{\vec{p}^2 + m^2}$  [5].

The eigenvalue equation reduces to a system of  $N$  mesh equations

$$\sum_{j=1}^N [T_{ij} + V(hx_i) \delta_{ij} - E \delta_{ij}] C_j = 0 \quad \text{with } C_j = \sqrt{h\lambda_j} u(hx_j), \quad (12)$$

where  $u(r)$  is the regularized radial wave function. The coefficients  $C_j$  provide the values of the radial wave function at mesh points. But contrary to some other mesh methods, the wave function is also known everywhere thanks to Eq. (4).

### III. THE MODELS

#### A. The relativistic flux tube

In the original RFT model [6], the meson is composed by two spinless particles—a quark and an antiquark—which move being attached with a flux tube. This tube is assumed to be linear with a uniform constant energy density  $a$  and carries angular momentum. A tube element has only a transverse velocity. The system rotates in a plane around the center of mass, assumed to be stationary. If  $r_i$  is the distance between the  $i$ th quark and the center of mass, and if we define  $\dot{r}_i = dr_i/dt$  the radial velocity of the  $i$ th quark, then the quark speed is given by  $v_i^2 = \dot{r}_i^2 + v_{i\perp}^2$ , where  $v_{i\perp}$  is its transverse velocity. We also assume that the energy density of the extremities of the flux tube is modified by a negative constant  $C/2$ , in order to take into account possible boundary effects due to the contact between the tube and the quark. Further, we consider that the quarks can interact via  $V(r)$  taking into account a short-range potential (a one-gluon-exchange process, for instance). These two extra terms are discussed in Ref. [8]. The Lagrangian  $\mathcal{L}$  of the meson is given by

$$\mathcal{L} = \mathcal{L}_1 + \mathcal{L}_2 - V(r), \quad (13)$$

$$\mathcal{L}_i = -m_i \gamma_i^{-1} - a \int_0^{r_i} dr'_i \gamma'_{i\perp}{}^{-1} - \frac{C}{2} \gamma_{i\perp}^{-1}, \quad (14)$$

where  $m_i$  is the constituent mass of the  $i$ th quark,  $\gamma_i = (1 - v_i^2)^{-1/2}$  and  $\gamma_{i\perp} = (1 - v_{i\perp}^2)^{-1/2}$ .

In the following, we will only consider the symmetric case,  $m_1 = m_2 \equiv m$ . Then  $r_1 = r_2$ , and  $r = 2r_1$ , and  $v_{1\perp} = v_{2\perp} = v_{\perp}$ . The corresponding quantized equations of the system are [6,8]

$$\frac{2\sqrt{\ell(\ell+1)}}{r} = \{v_{\perp} \gamma_{\perp}, W_r\} + a \{r, f(v_{\perp})\} + C v_{\perp} \gamma_{\perp}, \quad (15)$$

$$H = \{\gamma_{\perp}, W_r\} + \frac{a}{2} \left\{ r, \frac{\arcsin v_{\perp}}{v_{\perp}} \right\} + C \gamma_{\perp} + V(r), \quad (16)$$

where  $\ell$  is the orbital angular momentum,  $\{A, B\} = AB + BA$ ,  $4x^2 f(x) = \arcsin x - x\sqrt{1-x^2}$ ,  $W_r = \sqrt{p_r^2 + m^2}$ , and

$$p_r^2 \equiv - (1/r) (\partial^2 / \partial r^2) r.$$

The operator  $v_{\perp}$  commutes neither with  $r$  nor with  $p_r$  operators [6]. These equations reduce to a spinless Salpeter equation with the potential  $ar + V(r) + C$  when  $\ell=0$ , and to a

Schrödinger equation with the same potential in the nonrelativistic limit. The general case ( $m_1 \neq m_2$ ) is detailed in Ref. [7].

### B. The rotating string

Starting from the QCD Lagrangian and writing the gauge invariant  $q\bar{q}$  Green function for confined spinless quarks in the Feynman-Schwinger representation, one can arrive at the Nambu-Goto Lagrangian, which describes two quarks with masses  $m_1$  and  $m_2$ , attached by a string of energy density  $a$ . With the straight line ansatz and the introduction of auxiliary fields  $\mu_1$ ,  $\mu_2$ , and  $\nu$  (einbein fields) to get rid of the square roots appearing in this Lagrangian, one can obtain the Hamiltonian [11]

$$H = \frac{1}{2} \left[ \frac{p_r^2 + m_1^2}{\mu_1} + \frac{p_r^2 + m_2^2}{\mu_2} + \mu_1 + \mu_2 + a^2 r^2 \int_0^1 \frac{d\beta}{\nu} + \int_0^1 d\beta \nu + \frac{L^2}{a_3 r^2} \right] + V(r), \quad (17)$$

where

$$a_3 = \mu_1(1 - \zeta)^2 + \mu_2 \zeta^2 + \int_0^1 d\beta (\beta - \zeta)^2 \nu. \quad (18)$$

The potential  $V(r)$  takes into account interactions not simulated by the rotating string. We do not consider here a contribution coming from a constant potential  $C$ , as in the RFT model.  $L = \sqrt{\ell(\ell+1)}$  and  $\zeta$  defines the position  $R_\mu$  of the center of mass:  $R_\mu = \zeta x_{1\mu} + (1 - \zeta)x_{2\mu}$ , where  $x_{i\mu}$  is the coordinate of the  $i$ th quark, depending on the common proper time  $\tau$ . The string, with coordinate  $w_\mu$ , is described by two parameters on its worldsheet: one timelike  $\tau$  and one spacelike  $\beta$ . Within the straight line ansatz, the string coordinate is given by  $w_\mu = \beta x_{1\mu} + (1 - \beta)x_{2\mu}$ . The auxiliary fields  $\mu_1$  and  $\mu_2$  can be seen as effective masses of the quarks, while the auxiliary field  $\nu$  can be interpreted as an effective energy density for the string [9,11,12].

We are interested here in the resolution of the symmetrical case. When  $m_1 = m_2 = m$ , then  $\zeta = 1/2$  and  $\mu_1 = \mu_2 = \mu$ . Defining

$$y = \frac{L}{2a_3 r}, \quad (19)$$

one can eliminate  $\nu$  by a variation of the Hamiltonian. This extremal field  $\nu_0$  reads

$$\nu_0 = \frac{ar}{\sqrt{1 - 4y^2(\beta - 1/2)^2}}. \quad (20)$$

By replacing  $\nu$  by  $\nu_0$  in the Hamiltonian (17) and the relation (19), we obtain the following equations for the symmetrical rotating string [11]

$$\frac{\sqrt{\ell(\ell+1)}}{ar^2} = \frac{\mu y}{ar} + \frac{1}{4y^2} (\arcsin y - y\sqrt{1-y^2}), \quad (21)$$

$$H = \frac{p_r^2 + m^2}{\mu} + \mu + \frac{ar}{y} \arcsin y + \mu y^2 + V(r). \quad (22)$$

It has been shown in Ref. [12] that the extremal value of  $\mu$  giving  $\delta H / \delta \mu = 0$  is

$$\mu_0 = \sqrt{\frac{p_r^2 + m^2}{1 - y^2}}. \quad (23)$$

Moreover, the replacement of  $\mu$  by  $\mu_0$  in Eqs. (21) and (22) gives exactly the symmetrical RFT equations (15) and (16), with  $y$  equal to  $v_\perp$ . The RS model with all its auxiliary fields eliminated is thus equivalent to the RFT model in the classical symmetrical case. This is also true when ( $m_1 \neq m_2$ ), as shown in Ref. [13].

Here, we use the RS model with the auxiliary field  $\mu$  not eliminated, as in Refs. [9–11]. In these papers, the parameter  $\mu$  is considered as a real parameter and not as an operator. But, to avoid eventual singularities in the value of this auxiliary field when  $y$  is classically close to 1, we introduce explicitly the dependence of  $\mu$  in  $y$ , through the following substitution

$$\mu \rightarrow \frac{\rho}{\sqrt{1 - y^2}}, \quad (24)$$

where  $\rho$  is a real number. Such an expression is inspired by the result (23). As  $y$  is of the same nature as  $v_\perp$  in the RFT model, Eqs. (21) and (22) must be correctly symmetrized, and the quantized equations of the symmetrical rotating string are thus

$$\frac{\sqrt{\ell(\ell+1)}}{r} = \rho \frac{y}{\sqrt{1 - y^2}} + \frac{a}{2} \{r, f(y)\}, \quad (25)$$

$$H = \frac{1}{2\rho} \{p_r^2 + m^2, \sqrt{1 - y^2}\} + \rho \frac{1 + y^2}{\sqrt{1 - y^2}} + \frac{a}{2} \left\{ r, \frac{\arcsin y}{y} \right\} + V(r), \quad (26)$$

where  $4x^2 f(x) = \arcsin x - x\sqrt{1-x^2}$  like for the RFT model.

A particular solution depends on the value of this parameter  $\rho$ . Following Refs. [9,11], the physical value of  $\rho$  minimizes the mass of the state. The mean value  $\langle \mu \rangle = \langle \rho / \sqrt{1 - y^2} \rangle$  can be considered as a constituent mass for the quark, depending on the state. These equations reduce to a Schrödinger-like equation with the potential  $ar + V(r)$  when  $\ell = 0$  [12], and to a true Schrödinger equation with the same potential in the nonrelativistic limit.

## IV. RESOLUTION

### A. The relativistic flux tube

The main purpose of our work is the resolution of the symmetrical flux tube equations (15) and (16) using the Lagrange mesh method. To do this, we have to compute the matrix elements of the different operators in the Lagrange basis. As we consider a radial problem, we will use a Gauss-Laguerre quadrature. So, the corresponding Lagrange func-

tions will be given by Eq. (3). Let us define the different matrix elements we need to know

$$\begin{aligned}
 A_{ij} &= \left\langle f_i \left| \frac{2\sqrt{\ell(\ell+1)}}{r} \right| f_j \right\rangle, & B_{ij} &= \langle f_i | r | f_j \rangle, \\
 D_{ij} &= \langle f_i | W_r | f_j \rangle, \\
 F_{ij} &= \left\langle f_i \left| \frac{\arcsin v_\perp}{4v_\perp^2} - \frac{\sqrt{1-v_\perp^2}}{4v_\perp} \right| f_j \right\rangle, & G_{ij} &= \langle f_i | v_\perp \gamma_\perp | f_j \rangle, \\
 S_{ij} &= \left\langle f_i \left| \frac{\arcsin v_\perp}{v_\perp} \right| f_j \right\rangle, & \Gamma_{ij} &= \langle f_i | \gamma_\perp | f_j \rangle, \\
 V_{ij} &= \langle f_i | V(r) | f_j \rangle.
 \end{aligned} \tag{27}$$

With these notations, Eqs. (15) and (16) read

$$A = \{G, D\} + a\{B, F\} + CG, \tag{28}$$

$$H = \{\Gamma, D\} + \frac{a}{2}\{B, S\} + C\Gamma + V, \tag{29}$$

where we have used the approximate closure relation,

$$\sum_{k=1}^N |f_i\rangle\langle f_j| \approx 1, \tag{30}$$

to compute a product of two matrices.

The matrix elements  $A_{ij}$ ,  $B_{ij}$ , and  $V_{ij}$  are easy to compute, thanks to Eq. (6). Moreover, Eq. (9) gives us an analytical expression for  $p_{r,ij}^2$ , from which we can deduce the matrix elements  $D_{ij}$  by using the procedure described in Sec. II. The same procedure will allow us to compute  $F_{ij}$ ,  $G_{ij}$ ,  $S_{ij}$  and  $\Gamma_{ij}$  once the matrix elements of  $v_\perp$  are known. The determination of these matrix elements can be achieved by an iterative process, described here

(1) Equation (28) can be rewritten as

$$G = \frac{1}{2}\{P, D^{-1}\} - \frac{C}{2}\{G, D^{-1}\} - \frac{1}{2}DGD^{-1} - \frac{1}{2}D^{-1}GD, \tag{31}$$

where

$$P = A - a\{B, F\}. \tag{32}$$

This equation is symmetrized to ensure that  $G$  is Hermitian. It is worth noting that  $P = P(G)$  since  $F = F(G)$ . Starting from an known matrix  $G^k$  at the  $k$ th step,  $P^k$  can be computed and we obtain a new matrix  $G'^k$  with Eq. (31).

(2) This iterative process would diverge if we choose  $G^{k+1} = G'^k$ . So, we introduce a new parameter  $\epsilon < 1$  and define  $G^{k+1} = \epsilon G'^k + (1 - \epsilon)G^k$ .

(3) At each step  $k$ , the  $N$  eigenvalues  $\{v_{\perp,i}^{(k)}\}$  of the operator  $v_\perp$  are computed. The iteration procedure ends when

$$\frac{1}{N} \sum_{i=1}^N \left| \frac{v_{\perp,i}^{(k+1)} - v_{\perp,i}^{(k)}}{v_{\perp,i}^{(k+1)}} \right| < \eta, \tag{33}$$

where  $\eta$  is a fixed tolerance.

Once we have reached the convergence for  $G$ , we are able to compute  $S$  and  $\Gamma$ , which are now seen as functions of the matrix  $G$  rather than the matrix elements of the operator  $v_\perp$ . The Hamiltonian can then be computed and diagonalized.

Actually, the final matrix  $G$  is practically independent of the initial one  $G^0$ . However, the faster way to reach the convergence is to develop Eq. (15) at the first order in  $v_\perp$  and to choose the matrix  $G$  given by this development. At the first order,  $v_\perp \gamma_\perp \approx v_\perp$ , and

$$G^0 \approx \sqrt{\ell(\ell+1)} \left( \frac{1}{2}\{B, D\} + \frac{aB^2}{6} + \frac{C}{2} \right)^{-1}. \tag{34}$$

Let us note that a relevant starting matrix is obtained even if  $m=0$ .

## B. Rotating string

### 1. Lagrange mesh method

The resolution of the RS with the Lagrange mesh method is similar to that of the RFT. Indeed, using the previous definitions (27) with  $y$  instead of  $v_\perp$ , and defining

$$\begin{aligned}
 Q_{ij} &= \langle f_i | \sqrt{1-y^2} | f_j \rangle, & Y_{ij} &= \left\langle f_i \left| \frac{1+y^2}{\sqrt{1-y^2}} \right| f_j \right\rangle, \\
 E_{ij} &= \langle f_i | p_r^2 + m^2 | f_j \rangle,
 \end{aligned} \tag{35}$$

Eqs. (25) and (26) and are given by

$$G = \frac{1}{2\rho}(A - a\{B, F\}), \tag{36}$$

$$H = \frac{1}{2\rho}\{E, Q\} + \rho Y + \frac{a}{2}\{B, S\} + V. \tag{37}$$

Like for the RFT, we need to compute the matrix of the operator  $y$  to completely know the Hamiltonian. We will do this by an iterative process on  $G$  given directly by Eq. (36), with an initial value, obtained after a first order development, given by

$$G^0 = \sqrt{\ell(\ell+1)} \left( \rho B + \frac{a}{6} B^2 \right)^{-1}. \tag{38}$$

The last step in the resolution of the RS equations is always to find the value of the real number  $\rho$  realizing the minimum mass of a particular state. This extremal value is different for each state.

### 2. WKB method

Contrary to the case of the RFT, the operator  $p_r^2$  appears only in the equation defining the Hamiltonian for the RS. This makes possible a solution of Eqs. (25) and (26) and by a WKB method. Partial solutions of the RFT equations within this method are described in Ref. [15].

First, let us examine the case  $\ell=0$ . The RS equations reduce then to a spinless Salpeter equation of the form ( $\rho = \mu$  since  $y=0$ )

$$H = \frac{\vec{p}^2 + m^2}{\rho} + \rho + ar + V(r), \quad (39)$$

where

$$\vec{p}^2 = p_r^2 + \frac{L^2}{r^2}. \quad (40)$$

In the WKB method,  $L = \ell + 1/2$ . Consequently  $L^2 = 1/4$  here, and we obtain

$$p_r^2 = \rho M - \rho^2 - m^2 - \rho ar - \frac{1}{4r^2} - \rho V(r), \quad (41)$$

where  $M$  is the meson mass. We have then to compute  $r_+$  and  $r_-$  the two physical zeros of the classical quantity  $p_r^2$ . Finally, the resolution of the Bohr-Sommerfeld condition

$$\int_{r_-}^{r_+} p_r dr = \pi(n + \frac{1}{2}), \quad (42)$$

followed by a minimization of  $M$  with respect to the parameter  $\rho$  gives the mass of the state whose quantum numbers are  $\ell$  and  $n$ .

When  $\ell \neq 0$ , the WKB formulation of the classical RS equations (21) and (22), with the substitution (24), reads

$$\frac{\ell + \frac{1}{2}}{ar^2} = \frac{\rho y}{ar\sqrt{1-y^2}} + \frac{1}{4y^2}(\arcsin y - y\sqrt{1-y^2}), \quad (43)$$

$$M = \frac{1}{\rho}(p_r^2 + m^2)\sqrt{1-y^2} + \rho \frac{1+y^2}{\sqrt{1-y^2}} + \frac{ar}{y}\arcsin y + V(r). \quad (44)$$

The first one implicitly defines a function  $y = \tilde{y}(r, \ell, \rho)$ , which can be numerically computed. We can then formally write

$$p_r^2 = \frac{\rho}{\sqrt{1-\tilde{y}^2}} \left( M - V(r) - \frac{ar}{\tilde{y}} \arcsin \tilde{y} \right) - \rho^2 \frac{1+\tilde{y}^2}{1-\tilde{y}^2} - m^2. \quad (45)$$

The rest of the resolution is now identical to the previous case  $\ell=0$ .

## V. SET OF PARAMETERS

### A. Physical parameters

In this paper, we are mainly interested in the capacity of our method to give accurate solutions of the coupled equations for both RFT and RS models. But, in order to compare our results with previous studies and to use our method with physical parameters in interesting ranges, we will use the values of physical quantities from the models Ia and Ic developed in Ref. [8] (see Table I). Both models possess a Coulomb term with three values of the strength, depending on the quark content of the meson:  $\kappa_{hl}$  for heavy-light system,  $\kappa_{hh}$  for heavy-heavy system, and  $\kappa_{ll}$  for light-light system (light quark:  $u, d, s$ ; heavy quark:  $c, b$ ).

TABLE I. Two sets of physical parameters for the RFT and the RS models, from Ref. [8] ( $n=u$  or  $d$ ).

	Ia	Ic
$m_n$ (GeV)	0	0.233
$m_s$ (GeV)	0.317	0.416
$m_c$ (GeV)	1.456	1.658
$a$ (GeV <sup>2</sup> )	0.151	0.169
$C$ (GeV)	0	$-2m_n$
$\kappa_{ll}$	1.016	0.539
$\kappa_{hl}$	0.698	0.467
$\kappa_{hh}$	0.544	0.500

### B. The scale parameter

The Lagrange mesh method provides us a direct picture of the wave function at the mesh points. The best results are thus obtained when the mesh covers the main part of the wave function and the last mesh point is located in the asymptotic tail. That is why we are interested in an adequate determination of the scale parameter  $h$ . Since the method is not variational, no extremum of the mass can be expected for a defined value of  $h$  [5]. A good value for this quantity is given by  $h = r_a/x_N$ , where  $x_N$  is  $N$ th zero of the Laguerre polynomial (the last point of the mesh), and  $r_a$  represents a distance for which the asymptotic tail of the wave function is well defined. If  $x_N$  is well known,  $r_a$  is not. We show here how such a quantity can be estimated.

A typical evolution of the computed masses for different values of  $h$  is presented in Fig. 1. The existence of plateaus shows that the method does not require the knowledge of precise values of the scale parameter. A simple estimation will be sufficient, even to obtain accurate results.

For given quantum numbers, a system of two massless quarks is expected to have the maximal spatial extension,

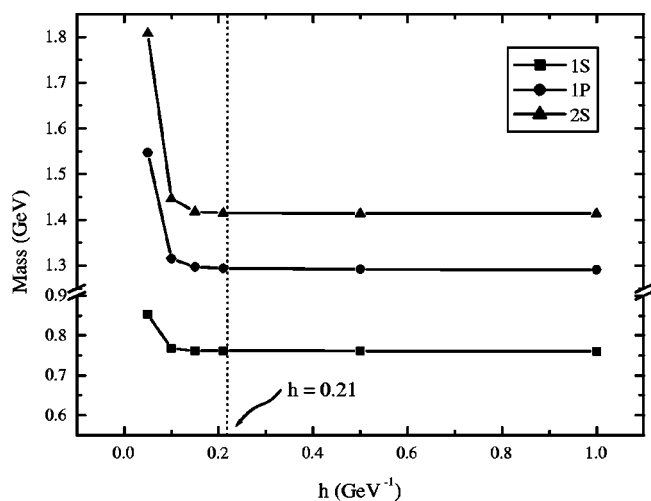


FIG. 1. Typical evolution of meson masses for the RFT model with the scale parameter  $h$ : 1S, 1P, and 2S states for the isospin 1 mesons, computed with the parameters Ia from Ref. [8]. Formula (53) gives  $h=0.21$  GeV<sup>-1</sup> for the 1S state; this value is correctly located in the plateau.

and so it could give an upper bound of the parameter  $h$ . First, we analyze the problem for the RS equations when  $\ell=0$ . These equations reduce then to a spinless Salpeter Hamiltonian, which reads

$$H_A = \frac{\vec{p}^2}{\rho} + \rho + ar. \quad (46)$$

We fix  $V(r)=0$ , since the asymptotic behavior is controlled by the confinement. The solutions have the following analytical forms ( $n=0,1, \dots$ ) [12]

$$E_{n0}(\rho) = \left(\frac{a^2}{\rho}\right)^{1/3} (-s_n) + \rho, \quad (47)$$

$$u_{n0}(r) = (\rho a)^{1/6} \frac{\text{Ai}((\rho a)^{1/3} r + s_n)}{|\text{Ai}'(s_n)|}, \quad (48)$$

where  $\text{Ai}(s)$  is the Airy function and  $s_n$  its  $n$ th zero, given by the approximate formula [16]

$$s_n \approx - \left[ \frac{3\pi}{2} \left( n + \frac{3}{4} \right) \right]^{2/3}. \quad (49)$$

Replacing  $\rho$  by its extremal value  $\rho_{n0}$ ,

$$\rho_{n0} = \sqrt{a} \left( \frac{-s_n}{3} \right)^{3/4}, \quad (50)$$

we have

$$u_{n0}(r) \propto \text{Ai} \left( \sqrt{a} \left( \frac{-s_n}{3} \right)^{1/4} r + s_n \right). \quad (51)$$

When  $s \approx 5$ ,  $\text{Ai}(s)$  is about 0.02% of its maximal value. Consequently, a good estimation of  $r_a$  is given by

$$\sqrt{a} \left( \frac{-s_n}{3} \right)^{1/4} r_a + s_n = 5. \quad (52)$$

At this point, we are able to compute a ‘‘physical’’ value for  $h$  when  $\ell=0$ . The extension of the wave function increases with the angular momentum. The simplest way to simulate such an increase is to compute  $r_a$  with the relation

$$\sqrt{a} \left( \frac{-s_{n+\ell}}{3} \right)^{1/4} r_a + s_{n+\ell} = 5. \quad (53)$$

This crude estimation of  $h$  is satisfactory because it is always located in the plateau. Moreover, we will use it in both RFT and RS methods, because of the classical equivalence between these two theories.

### C. Numerical parameters

The accuracy of the solutions depends mainly on two parameters: the number  $N$  of mesh points (basis states) and the value of the tolerance  $\eta$  on the eigenvalues of the operator  $v_\perp$ . For instance, a relative error on meson masses around  $10^{-5}$  can be reached with  $N \geq 30$  and  $\eta \leq 10^{-6}$ . The accuracy can be increased by using greater values of  $N$  and smaller values of  $\eta$ .

TABLE II. Approximate optimal values for the parameter  $\epsilon$  in different cases.

$m/\sqrt{a}$	$\epsilon$	
	RFT	RS
$\approx 0$	0.005	0.1
$\geq 1$	0.01	0.1

If the value of the mixing parameters  $\epsilon$  is too high, the iterative process diverges. The best value of  $\epsilon$  is chosen as the largest value for which the process converges. It depends on the case considered, as shown in Table II. It clearly appears that the iterative process does not converge easily with the RFT equations, especially when the quarks are massless. About 700 iterations are needed in this case, and 400 when  $m/\sqrt{a} \geq 1$ . However, the RS solutions converge faster, and one can reach the convergence after about only 40 iterations.

## VI. RESULTS

### A. Relativistic flux tube

The Lagrange mesh method is not variational. But, in practice for a sufficiently high number of basis states, the method is often variational (eigenvalues computed are all upper bounds) or antivariational (eigenvalues computed are all lower bounds) [5].

We have computed with the Lagrange mesh method the solutions of the RFT equations for models Ia and Ic from Ref. [8] (see Table I). All the masses are computed with  $N = 30$ ,  $\eta = 10^{-6}$ , the scale parameter  $h$  is estimated thanks to Eq. (53), and the parameter  $\epsilon$  is taken from Table II. Meson masses are presented in Table III with the corresponding ones computed with the method developed in Ref. [8], relying on a harmonic oscillator basis. Experimental data are given in order to show that the parameters used are physically relevant.

The results of both methods are compatible. Nevertheless, the masses computed with the Lagrange mesh method are always smaller than the masses computed with the harmonic oscillator method, although the Lagrange mesh method is not variational. We obtain similar results when both methods are used to solve ordinary Schrödinger and spinless Salpeter equations. We have thus strong confidence in our new method to provide a better convergence of the results. The improvement is especially important for light quark masses. Differences between the two methods vanish when the quark mass increases.

It is worth noting that the masses computed with method of Ref. [8] are strongly dependent of the values chosen for the oscillator length. So a supplementary minimization on this parameter, for each state, is necessary to obtain the optimal value of a mass. This is not necessary with the Lagrange mesh method since it is nearly independent of the scale parameter (see Fig. 1).

The small differences between the masses obtained with the Lagrange mesh method and the harmonic oscillator method are a strong indication that our method works well.

TABLE III. Meson masses for the RFT model, with two sets Ia and Ic of parameters from Ref. [8], computed using the Lagrange mesh method (Lag.) and a previous technique relying on an harmonic oscillator basis (HO) [8]. The experimental masses (Expt.) are given, without error, for information.

		Mass (Gev)				
	$(n+1)^{2S+1}L_J$	Expt.	HO (Ia)	Lag.(Ia)	HO (Ic)	Lag. (Ic)
$n\bar{n}$	$1^3S_1$	0.771	0.781	0.762	0.774	0.773
	$1^3S_1$	1.318	1.310	1.300	1.320	1.319
	$1^3D_3$	1.691	1.654	1.643	1.689	1.676
	$2^3S_1$	1.465	1.450	1.415	1.427	1.424
	$2^3P_2$	1.810	1.841	1.832	1.797	1.794
$s\bar{s}$	$1^3S_1$	1.019	0.988	0.968	1.010	1.010
	$1^3P_2$	1.525	1.540	1.534	1.517	1.515
	$1^3D_1$	1.854	1.881	1.877	1.867	1.865
	$2^3S_1$	1.680	1.671	1.641	1.644	1.641
	$2^3P_2$	2.011	2.053	2.047	1.994	1.991
$c\bar{c}$	$1^3S_1$	3.097	3.131	3.130	3.116	3.115
	$1^3P_2$	3.556	3.528	3.527	3.542	3.542
	$1^3D_3$	3.770	3.788	3.788	3.820	3.820
	$2^3S_1$	3.686	3.666	3.663	3.664	3.661
	$2^3D_1$	4.159	4.128	4.128	4.165	4.164

But we want another test. It will be given by the study of the RS model.

### B. Rotating string

Solutions of the RS equations computed with the Lagrange mesh method (numerical parameters as in Sec. VI A) and the WKB approximation are presented in Table IV. The masses are obtained using the set Ia of parameters (see Table I), for a pure string without Coulomb-like potential.

The two methods to solve the RS equations lead to very close results. This shows that the semiclassical approximation is efficient in this case, but also that the Lagrange mesh method works correctly. Figure 2 shows the existence of a

TABLE IV. Meson masses for the RS model computed with the Lagrange mesh method and the WKB approximation. The interaction Ia from Ref. [8] is used, but without the Coulomb potential. The extremal value  $\rho_0$ , to the nearest 10 MeV, of the parameter  $\rho$  is given in both cases.

		Lagrange mesh		WKB	
		Mass (GeV)	$\rho_0$ (GeV)	Mass (GeV)	$\rho_0$ (GeV)
$n\bar{n}$	$1^3S_1$	1.289	0.32	1.294	0.32
	$1^3P_2$	1.581	0.16	1.589	0.16
	$2^3S_1$	1.960	0.49	1.963	0.49
$c\bar{c}$	$1^3S_1$	3.492	1.55	3.493	1.55
	$1^3P_2$	3.731	1.52	3.730	1.51
	$2^3S_1$	3.916	1.65	3.917	1.65

minimal mass for a particular value  $\rho_0$  of the parameter  $\rho$  in the RS equations. In our calculations,  $\rho_0$  has been determined to the nearest 10 MeV, and is the same in the two methods with that precision. An accuracy below 1 MeV is then reached for the masses.

### C. Comparison between RFT and RS

If the RS model is classically equivalent to the RFT model once the auxiliary fields are correctly eliminated, the two models should not give the same results when a real parameter  $\rho$  is kept in the RS equations. In a previous study

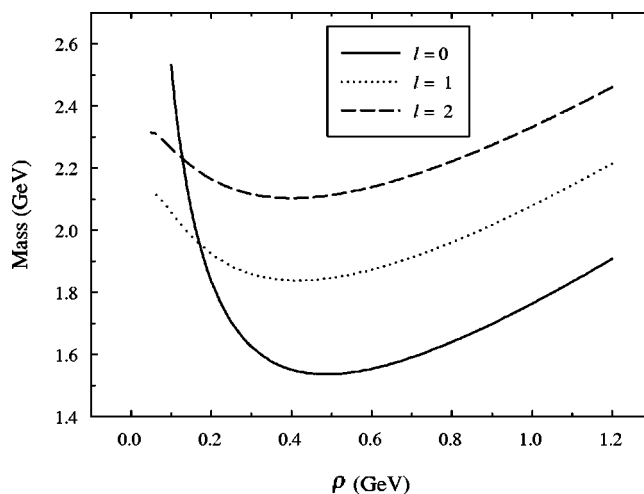


FIG. 2. Meson masses for the RS model, computed with the Lagrange mesh method, versus the parameter  $\rho$ :  $1S$ ,  $1P$ , and  $1D$  states for the  $s\bar{s}$  system, computed with the interaction Ia from Ref. [8], but without the Coulomb potential.

TABLE V. Meson masses computed with the Lagrange mesh method within the RFT and the RS models. The interaction Ia from Ref. [8] is used, but without the Coulomb potential. The values of the effective masses  $\mu_0$  and  $\mu_{\text{RFT}}$  are given.

		Relativistic flux tube		Rotating string	
		Mass (GeV)	$\mu_{\text{RFT}}$ (GeV)	Mass (GeV)	$\mu_0$ (GeV)
$n\bar{n}$	$1^3S_1$	1.228	0.308	1.289	0.32
	$1^3P_2$	1.543	0.323	1.581	0.29
	$1^3D_3$	1.825	0.342	1.860	0.32
	$2^3S_1$	1.832	0.460	1.960	0.49
	$2^3P_2$	2.071	0.498	2.155	0.49
$s\bar{s}$	$1^3S_1$	1.507	0.486	1.536	0.49
	$1^3P_2$	1.809	0.523	1.838	0.52
	$1^3D_3$	2.078	0.593	2.103	0.56
	$2^3S_1$	2.070	0.612	2.142	0.62
	$2^3P_2$	2.294	0.647	2.343	0.64
$c\bar{c}$	$1^3S_1$	3.486	1.555	3.492	1.55
	$1^3P_2$	3.723	1.594	3.731	1.58
	$1^3D_3$	3.931	1.625	3.937	1.62
	$2^3S_1$	3.902	1.631	3.916	1.65
	$2^3P_2$	4.081	1.661	4.094	1.66

[12], some results have been obtained about the equivalence between a spinless Salpeter Hamiltonian  $H_{SS}$  and a corresponding Hamiltonian with auxiliary field  $H_A$ : the eigenvalues of  $H_A$  are upper bounds of the eigenvalues of  $H_{SS}$  [17] with relative differences around 7% for the lowest states. We know that the RFT and RS equations reduce, respectively, to eigenvalue equations for Hamiltonians  $H_{SS}$  and  $H_A$  for a vanishing angular momentum. It should be interesting to see if there is the same kind of relation between the masses for the RFT and RS models when  $\ell \neq 0$ .

Another result can be expected: once we know an eigenfunction  $|\psi_{\text{RS}}\rangle$  of the RS Hamiltonian for the extremal value  $\rho_0$ , we are able to compute the effective mass  $\mu_0 = \rho_0 \langle 1/\sqrt{1-y^2} \rangle$  for this state. This quantity should be

approximately equal to the mean value  $\mu_{\text{RFT}} = \langle \sqrt{(p_r^2 + m^2)/(1-v_\perp^2)} \rangle$  for the corresponding state  $|\psi_{\text{RFT}}\rangle$ , due to the equivalence between the two models via Eq. (23).

Our results are given in Table V. The masses for both RFT and RS models are computed with the Lagrange mesh method for the same parameters as in Sec. VI B. The RS masses are always upper bounds of the RFT masses with relative differences around by 7%, as in the limiting case of vanishing angular momentum. We also see that  $\mu_{\text{RFT}} \approx \mu_0$  as expected. We can finally notice that the results of the two models are closer and closer when the mass of the constituent quark increases, because the RFT and the RS model possess a common nonrelativistic limit: the Schrödinger equation with a linear potential.

## VII. CONCLUSIONS

We have shown in this paper that the Lagrange mesh method can be used to solve successfully the equations of the relativistic flux tube model in the symmetrical case. The masses obtained are in good agreement with a previous resolution in a harmonic oscillator basis [8]. But the Lagrange mesh method is more efficient, due to its independence of the scale parameter used to fit the size of the trial states. Moreover, a better convergence is reached. This proves the validity of our method.

We have also solved the equations of the symmetrical rotating string model with the Lagrange mesh method and with the WKB approximation. The masses computed with these two procedures are very close, showing that the Lagrange mesh method correctly works, and that the WKB approximation is efficient here. If we compare the masses given by the relativistic flux tube and the rotating string models, we find relative differences around 7% for the lowest states, as expected because the two models are classically equivalent. This point is a last confirmation of the relevance of the Lagrange mesh method to solve the relativistic flux tube equations.

## ACKNOWLEDGMENT

C.S. and F.B. thank the FNRS for financial support.

- 
- [1] D. Baye and P.-H. Heenen, J. Phys. A **19**, 2041 (1986).  
[2] M. Vincke, L. Malegat, and D. Baye, J. Phys. B **26**, 811 (1993).  
[3] D. Baye, J. Phys. B **28**, 4399 (1995).  
[4] M. Hesse and D. Baye, J. Phys. B **32**, 5605 (1999).  
[5] C. Semay, D. Baye, M. Hesse, and B. Silvestre-Brac, Phys. Rev. E **64**, 016703 (2001).  
[6] D. LaCourse and M. G. Olsson, Phys. Rev. D **39**, 2751 (1989).  
[7] M. G. Olsson and Siniša Veseli, Phys. Rev. D **51**, 3578 (1995).  
[8] C. Semay and B. Silvestre-Brac, Phys. Rev. D **52**, 6553 (1995).  
[9] A. Yu. Dubin, A. B. Kaidalov, and Yu. A. Simonov, Phys. Lett. B **323**, 41 (1994).  
[10] E. L. Gubankova and A. Yu. Dubin, Phys. Lett. B **334**, 180 (1994).  
[11] V. L. Morgunov, A. V. Nefediev, and Yu. A. Simonov, Phys. Lett. B **459**, 653 (1999).  
[12] C. Semay, B. Silvestre-Brac, and I. M. Narodetskii, Phys. Rev. D **69**, 014003 (2004).  
[13] F. Buisseret and C. Semay, Phys. Rev. D **70**, 077501 (2004).  
[14] D. Baye, M. Hesse, and M. Vincke, Phys. Rev. E **65**, 026701 (2002).  
[15] T. J. Allen, C. Goebel, M. G. Olsson, and Siniša Veseli, Phys. Rev. D **64**, 094011 (2001).  
[16] M. Abramowitz and I. A. Stegun, *Handbook of Mathematical Functions* (Dover, New York, 1970).  
[17] W. Lucha and F. F. Schöberl, Phys. Rev. A **54**, 3790 (1996).